CHAPTER 4 : OPTICAL PROPERTIES- RESULTS AND DISCUSSION

4.1 Introduction

Understanding of optical characteristics of materials is important if the material is to be used as optical elements. It is therefore important to characterize the optical constants (the refractive index, n and the extinction coefficient, k) of the film and to determine the their thickness, t. The optical constants are sensitive to the microstructure which is affected by the deposition conditions[81-83]. A good knowledge of film parameters is necessary for the design and manufacture of new optical coatings and devices such as light emitting diodes [84,85] and heterojunction solar cells [86].

The reflectance and transmittance measurement method is one of the most powerful techniques for the determination of optical constants and thickness [87]; it measures reflectance, R and/or transmittance, T of thin films by means of wavelengths and incident angles of illuminating light. In the present study, transmission data obtained from UV-VIS-NIR spectrophotometer was used to determine optical constants of CdTe thin films. A method of calculation which is a combination of methods proposed by Cisneros [88] and Davis et.al [89] was developed and employed. The results obtained compare very well with the published data on CdTe thin films prepared by various other techniques[6,49,52].

4.2 Principles of the method

Conventional optical methods for determining the optical constants and thickness as employed by several researches [87,88,89,90-98] can be summarized as follows

$$T \equiv T\,(n, k, t, \lambda)$$

$$R \equiv R\,(n, k, t, \lambda),$$

where T and R are the spectral transmittance and reflectance respective of a film and λ is the wavelength of the incident light. It is to be noted that the conventional methods mentioned above always lead to multiple solutions [99,100] and to choose the correct solution an efficient criterion has to be applied [101,102].

Figure 4.1 represent a thin film with a complex refractive index, $n_2^* = n - ik$, bounded by two transparent media with refractive indices n_1 and n_3.

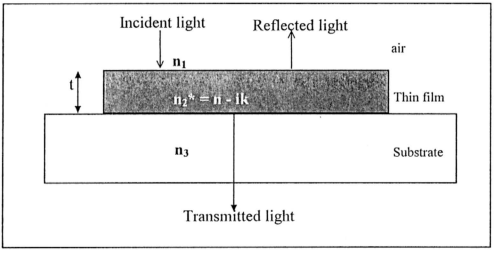

Figure 4.1 : Transmission and reflection of light by a single thin film

(t = thickness of thin film; n_1 = refractive index of air; n_3 = refractive index of substrate; n_2^* = complex refractive index of thin film; k = extinction coefficient)

The transmittance and reflectance normal to the incident film are given by

$$T = \frac{n_1}{n_3}\left|\frac{t_{32}t_{12}\exp(i\beta)}{1 + r_{32}r_{12}\exp(i2\beta)}\right|^2 \qquad \ldots\ldots\ldots (4.1)$$

$$R = \left| \frac{r_{12} + r_{23} \exp(i2\beta)}{1 + r_{12} r_{23} \exp(i2\beta)} \right|^2 \qquad \ldots\ldots\ldots (4.2)$$

The indices 1,2 and 3 correspond to air, film and substrate respectively; r_{ij} and t_{ij} are Fresnel coefficients which for normal incidence are

$$t_{ij} = \frac{2N_i}{N_i + N_j} \qquad \ldots\ldots\ldots (4.3)$$

$$r_{ij} = \frac{N_i - N_j}{N_i + N_j} \qquad \ldots\ldots\ldots (4.4)$$

Taking $N_2 = n + ik$ with n and k real functions of λ, the complex angle β is given by

$$\beta = \frac{2\pi \, t\, N}{\lambda} = \frac{2\pi \, tn}{\lambda} + i\frac{2\pi \, tk}{\lambda} \qquad \ldots\ldots\ldots (4.5)$$

where t is the film thickness and λ is the vacuum wavelength of the incident radiation.

Since the surrounding media (glass and air) is assumed to be transparent, N_1 and N_3 are real quantities and which are represented by n_1 and n_3. By replacing Fresnel coefficient (equation 4.3) into equation 4.1 and considering a weak absorption i.e. $k^2 << (n_2-n_1)^2$ and $k^2 << (n_2-n_3)^2$, equation 4.1 can be approximated to

$$T = \frac{16 n_1 n_3 n^2 A}{C_1^2 + C_2^2 A^2 + 2C_1 C_2 A \cos\left(\frac{4\pi \, nt}{\lambda}\right)} \qquad \ldots\ldots\ldots (4.6)$$

where $C_1 = (n + n_1)(n + n_3)$; $C_2 = (n - n_1)(n_3 - n)$ and $A = \exp(-4\pi kt/\lambda) = \exp(-\alpha t)$, where α = absorption coefficient = $4\pi k/\lambda$.

4.3 Determination of optical thickness, d.

A typical transmission spectrum for thin film CdTe is shown in figure 4.2. the fall in transmittance at about 850 nm is corresponding to the fundamental absorption

edge. At longer wavelengths, the film is essentially transparent (where R+T = 1) and large interference fringes are obtained in T.

The interference maxima shown in figure 4.2 can be used to determine the optical thickness, d, as proposed by Cisneros [88] . At extreme points the derivative of transmittance, T, takes the form

$$\frac{dT}{d\lambda} = 0$$

which satisfies the condition

$$\frac{4\pi d}{\lambda_m} = m\pi \qquad \ldots\ldots (4.7)$$

where d = optical thickness = nt $\qquad \ldots\ldots (4.8)$

and m = 1,2,3,…., is the order number and λ_m is the wavelength corresponding to the extremum of order m.

Assuming small variations in the optical thickness from one extremum to the nearest neighbor, we have

$$d_{m-1} \approx d_m \approx d_{m+1}$$

or $$(m-1)\,\lambda_{m-1} \approx m\lambda_m \approx (m+1)\,\lambda_{m+1} \ldots\ldots (4.9)$$

Consequently the following alternative formulae for m is obtained.

$$m \approx \frac{\lambda_{m-1}}{\lambda_{m-1} - \lambda_m} \qquad \ldots\ldots (4.10a)$$

$$m \approx \frac{\lambda_{m+1}}{\lambda_m - \lambda_{m+1}} \qquad \ldots\ldots (4.10b)$$

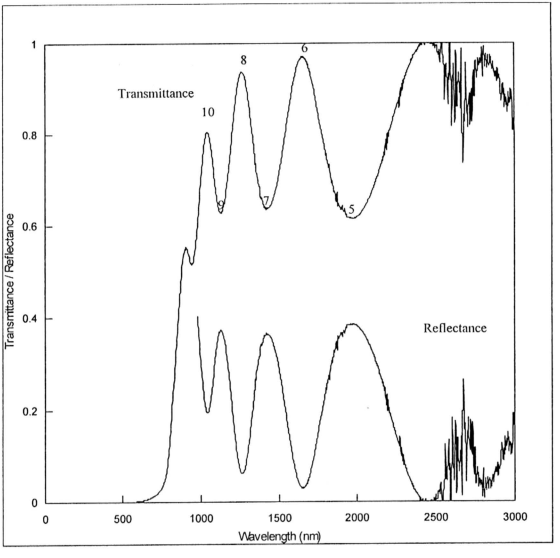

Figure 4.2 : Typical transmittance spectra of thin film CdTe prepared by e-beam evaporation.

(In the figure is also shown the spectra for reflectance which was calculated for long wavelength region using the assumption R + T = 1; numbers at the extremum refers to the order numbers as tabulated in table 4.1)

$$m \approx \frac{\lambda_{m-1} + \lambda_{m+1}}{\lambda_{m-1} - \lambda_{m+1}} \qquad \ldots\ldots\ldots (4.10c)$$

Using the approximate values given by equation 4.10 and the fact that the order of the maxima and minima have definite and opposite parities, we can choose the correct integer values of m. Consequently, the first approximation of the optical thickness at extrema can be calculated from

$$d_m = \frac{m\lambda_m}{4} \qquad \ldots\ldots\ldots (4.11)$$

An example of calculation is shown in table 4.1 for sample b21776ct.

Table 4.1 : Determination of the order numbers and optical thickness

λ_m (nm)	m (eqn.10a)	m (eqn.10b)	m (eqn.(10c)	average m	d_m (nm)
2270	-	5.52	-	5	2838
1922	6.52	7.63	6.57	6	2883
1670	7.63	7.43	7.54	7	2923
1472	8.43	8.09	8.28	8	2944
1310	9.09	11.03	9.9	9	2948
1202	12.13	10.56	11.36	10	3005
1098	11.56	13.8	12.51	11	3020

4.4 Determination of refractive index, geometrical thickness and extinction coefficient, k.

Assuming both the film and the substrate to be transparent and non-absorbing in the long wavelength region, we can come to a condition that the reflectivity, R and transmission, T of the film plus the substrate combination be unity (i.e. R + T = 1) [89]. Under this condition the values of the reflectivity at the extrema (R_{min} and R_{max}) of the interference fringes are given by

$$R_{even} = \left(\frac{n_1 - n_3}{n_1 + n_3}\right)^2 \qquad \ldots\ldots\ldots (4.12\ a)$$

$$R_{odd} = \left(\frac{n_3 - n}{n_3 + n}\right)^2 \qquad \ldots\ldots\ldots (4.12\ b)$$

where 'even' and 'odd' correspond to the order of the fringes and n_3 is the refractive index of the substrate. In these equations, maxima occur for odd integer order where $R_{max} > R_{substrate}$ and for even integer orders when $R_{min} < R_{substrate}$ since $R_{even} = R_{substrate}$.

Davis [9] showed that $R_{odd} = R_{max}$, and it can be written as

$$R^{\frac{1}{2}} = \pm\frac{(n_3 - n^2)}{(n_3 + n^2)}$$

and the positive roots of this equation are

$$n' = \sqrt{n_3\left(\frac{1 - R_{max}^{1/2}}{1 + R_{max}^{1/2}}\right)} \qquad \ldots\ldots\ldots (4.13)$$

$$n'' = \frac{n_3}{n'} \qquad \ldots\ldots\ldots (4.14)$$

In order to choose the best solution, a criterion was adapted. The value of n' was chosen if $n' > 1$ and $n'' < n_3$, as n is usually greater than unity for the frequencies used in optical work. In the present work, as reflectivity measurement was not done, the values at the extrema for reflectivity were obtained from the transmission data by using the assumption $R + T = 1$, which obeys very well for long wavelength region (as seen in the figure 4.2).

From the value of optical thickness, d and refractive index calculated from equation 4.13 at the extrema, geometrical thickness was calculated (using equation 4.12). By taking the assumption that thickness, t, is constant for the entire range of wavelength, an average value of t was obtained. Consecutively, refractive index was recalculated for these extrema points from equation 4.8. A sample calculation is shown in table 4.2.

Table 4.2 : Refractive index and geometrical thickness

Wavelength (nm)	R_{max} (R_{max}=1-T_{min})	Refractive index, n(=n')	geometrical thickness, t (nm)	refractive index (recalculated)
2270	0.42	2.67	1062	2.75
1670	0.42	2.67	1095	2.79
1310	0.43	2.70	1092	2.83
1098	0.48	2.89	1045	2.85

The value of n obtained from this calculation was fitted to Cauchy relationship given by

$$n^2 = A + B/\lambda^2 + \ldots\ldots \qquad \ldots\ldots\ldots (4.15)$$

The behavior of n, depends on the constants A and B.

Using the approach T (n, k, t, λ) - T_{exp} = 0, we obtain for low absorbing region

$$\frac{16n_1n_3n^2A}{C_1^2 + C_2^2 + 2C_1C_2A\cos\left(\frac{4\pi\,nt}{\lambda}\right)} = T_{exp} = T \quad \ldots\ldots\ldots (4.16)$$

where T_{exp} = T = transmittance value obtained from experiment. This equation can be rewritten as

$$\left(C_2^2T\right)A^2 + \left(2C_1C_2T\cos\left[\frac{4\pi\,nt}{\lambda}\right] - 16n_1n_3n^2\right)A + C_1^2T = 0 \ldots (4.17)$$

The roots of this equation are

$$A = \frac{-\left(2C_1C_2T\cos\left[\frac{4\pi nt}{\lambda}\right] - 16n_1n_3n^2\right) \pm \left\{\left[2C_1C_2T\cos\left[\frac{4\pi nt}{\lambda}\right] - 16n_1n_3n^2\right]^2 - \left[4T^2C_1^2C_2^2\right]\right\}^{1/2}}{2TC_2^2}$$

.....(4.18)

The calculated values of n, t with the T_{exp} at a particular λ were used to estimate A. The criteria used to choose the correct value for A was that 0<A<1. From the value of A, the extinction coefficient, k was calculated by

$$k = \frac{-\lambda}{4\pi\,nt}\ln A \quad \ldots\ldots (4.19)$$

The calculated values of n and thickness, t were substituted into equation 4.6 to calculate transmittance, T_{cal}, along the low absorption region by assuming zero absorption (k = 0). The calculated values were plotted along with the experimental values of transmittance to show their dependency. A good fit was seen as shown in figure 4.3 indicating an excellent accuracy in the method of calculation employed. The

calculated values for constants A and B together with thickness are tabulated in table 4.3

Table 4.3 : Fitting parameters and film thickness

sample	A	B $(\mu m)^2$	thickness, t (nm)
b21771ct	7.55	1.1	1056
b21772ct	7.5	1.2	923
b21773ct	7.21	1.01	1069
b21774ct	8.18	1.01	1071
b21775ct	7.91	0.11	1009
b21777ct	7.16	1.70	1040
b21778ct	7.07	1.44	861.1
b3861ct	11.5	0.95	648.5
b3862ct	7.76	0.93	838.9
b3863ct	7.85	0.42	757
b3864ct	8.10	1.40	790
b3865ct	7.93	0.88	728
b3686ct	7.34	0.60	755
b3687ct	7.63	1.20	823.9
b3688ct	8.33	1.50	771.5
b41381ct	5.65	1.18	558.1
b41382ct	6.40	0.89	581
b41383ct	6.10	0.40	609
b41384ct	6.20	0.25	549
b41385ct	5.81	0.89	591.1
b41386ct	6.21	0.30	629.1
b41387ct	6.62	0.29	594.7
b41388ct	6.21	0.11	564
b62591ct	6.72	0.90	1045.4
b62592ct	6.68	0.39	1150
b62593ct	5.98	0.05	1161.1
b62594ct	6.41	0.56	917.9
b62595ct	6.11	1.49	920
b62596ct	5.52	1.86	1114.1
b62597ct	6.21	1.20	1011.1
b62598ct	6.11	0.40	1169.1

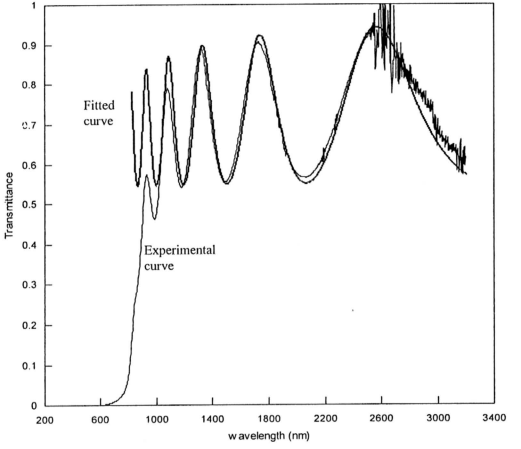

Figure 4.3 : Comparison between the transmission curve of CdTe thin film and the fitted curve.

4.5 Dispersion of refractive index, n and the extinction coefficient, k

Figure 4.4 shows the dispersion of refractive index of electron-beam evaporated CdTe thin film with wavelength. It also shows the comparison in the dispersion for films with different thickness. The refractive index increases near the absorption edge (~950 nm), showing a normal dispersion. Beyond this edge (>950 nm), the refractive index, n, approaches a constant value. All the other films prepared showed similar behavior.

The values of n obtained in this work for CdTe thin films are in reasonable agreement with the published data where n takes a value of 2.5 - 2.7 for wavelength ≥ 1200 nm [6,45,52,103,104] as shown in figure 4.4. Films with increasing thickness show an increase in the refractive index value beyond the absorption edge. This behavior is attributed to an increase in the crystallinity of the deposited films. This behavior is also consistent with the structural investigations reported in chapter 3, where the crystallite size increases with film thickness. Low values of refractive index in very thin films, might be also due to the discontinuity of the film in the first stages [45]. As the film grows, the continuity is improved and coupled with the increasing crystallinity, causes the increase in the refractive index as observed.

An anomalous behavior is observed in the dispersion of the refractive index near the band edge. No single pattern is observed as films showed varying curvature near the absorption edge irrespective of their thickness. The curvature was expected to increase with increasing crytsallinity, i.e. increasing thickness. The anomalous behavior

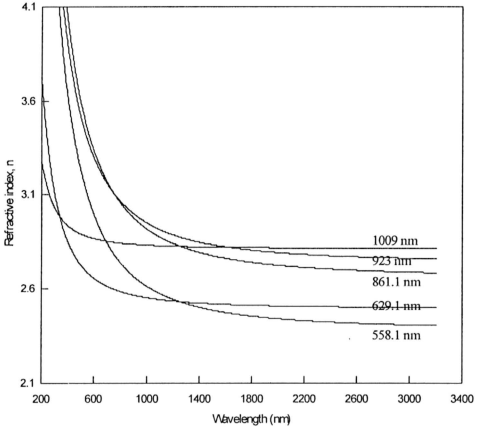

Figure 4.4 : Dispersion of refractive index of e-beam evaporated CdTe thin films with different thickness.
(Refractive index increases with film thickness; the film thickness are shown at the end of each curve)

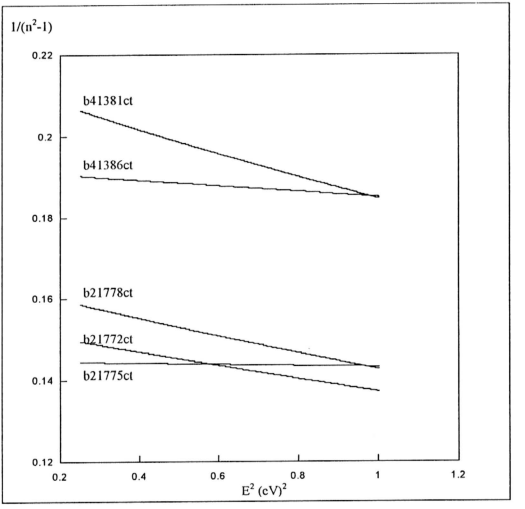

Figure 4.5 : $1/(n^2-1)$ vs. E^2

Comparing equation 4.20 and 4.21, the plasma energy E_p ($=\hbar\omega_p$) at which the valence electrons are freed from their nuclei and thus the plasma frequency can be calculated. The valence electron density in a solid, N_v, is calculated using

$$(\omega_p)^2 = \frac{4\pi N_v e^2}{m_e} \qquad \text{..... (4.22)}$$

The calculated values are tabulated in table 4.4.

Dispersion data as reported [29] for bulk CdTe were 3.78 eV for average oscillator strength, E_o and 23.4 eV for a dispersion energy, E_d. The values obtained for both the oscillator and the dispersion energies were larger than the quoted values in reference 29. The dispersion energy obeys an empirical relationship

$$E_d = \beta N_c Z_a N_e (eV) \qquad \text{..... (4.23)}$$

where N_c, Z_a and N_e are the co-ordination number of the cation, chemical valency of the anion and the total number of valence electrons per anion respectively. As such, disorder or impurities present in the film could alter the value of the oscillator and dispersion energies of the polycrystalline thin films as these material are sensitive to preparation techniques than is the case for single crystals.

The spectral variation of the extinction coefficient, k is represented in the figure 4.6. It shows that the absorption in all the films starts below 850 nm. The absorption edge varies for film with different thickness, due to the presence of crystallites with varying sizes. The extinction coefficient, k decreases with film thickness indicating a strong absorption in thick films, which is again due to the presence of large crystallites.

Table 4.4 : Dispersion energy, oscillator strength, plasma energy and valence electron density

sample	Oscillator strength, E_o (eV)	Dispersion energy, E_d (eV)	Plasma energy, E_p (eV)	Electron Density, N_v ($x10^{22}/cm^3$)
b21771ct	3.19	21.91	8.17	3.51
b21772ct	3.05	19.9	7.79	3.34
b21773ct	3.26	20.58	8.19	3.52
b21774ct	3.45	24.82	6.26	2.67
b21775ct	9.82	67.88	25.82	11.08
b21777ct	2.56	15.87	6.38	2.74
b21778ct	2.73	16.66	6.75	2.90
b3861ct	4.24	44.57	13.75	5.90
b3862ct	3.49	23.63	9.09	3.90
b3863ct	5.11	34.98	13.36	5.73
b3864ct	2.97	21.14	7.91	3.40
b3865ct	3.62	25.10	9.53	4.09
b3686ct	4.15	23.35	10.46	4.19
b3687ct	9.74	64.74	25.11	10.78
b3688ct	2.92	21.43	7.91	3.40
b41381ct	2.66	12.41	5.75	2.47
b41382ct	3.21	17.39	7.47	3.21
b41383ct	4.54	23.17	10.26	4.40
b41384ct	5.75	29.92	13.12	5.63
b41385ct	3.05	14.72	6.70	2.88
b41386ct	5.25	27.34	11.98	5.14
b41387ct	5.52	31.06	13.09	5.62
b41388ct	8.62	44.94	19.68	8.45
b62591ct	3.27	18.75	7.83	3.36
b62592ct	4.85	27.58	11.57	4.97
b62593ct	12.29	61.19	27.42	11.77
b62594ct	3.97	21.51	9.24	3.97
b62595ct	2.50	12.87	5.67	2.43
b62596ct	2.80	9.94	4.66	2.00
b62597ct	2.76	14.44	6.31	2.71
b62598ct	4.54	23.20	10.26	4.40

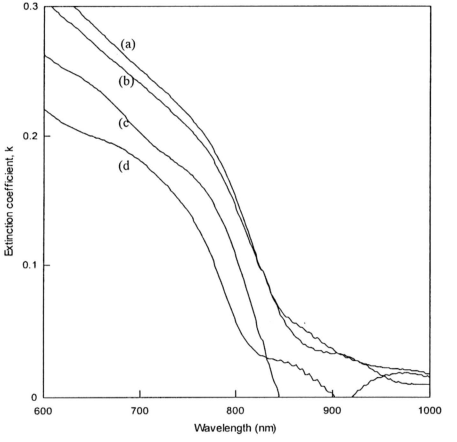

Figure 4.6 : Dispersion of extinction coefficient

[(a) t= 923 nm; (b) t=861 nm; (c) t=629 nm; (d) t=558.1 nm]

Such a dependence of optical constants (n,k) on the film thickness and also substrate temperature have been reported elsewhere [107]. This behavior had been reported [45,48] to be influenced by the presence of free tellurium in the thin film, that is the stoichiometry of the thin film. Films grown at high substrate temperature show the expected ratio, 1:1 [48], while those grown at lower temperatures as in the present study, show rich tellurium in the thin film. This variation leads to the anomalous dispersion observed in the behavior of optical constants. It is concluded that not only the crystallite size has an effect on the behavior of optical constants but also the stoichiometry.

4.6 Absorption coefficient, α and evaluation of band gap

Calculation of fundamental band gap is a tedious work as it is influenced by many factors such as temperature, structural modifications etc. Two methods are widely used in the determination of band gap, the first is the fitting of the α, to a theoretical methods of direct and indirect dipolar transitions between parabolic bands [86,109,110] and the other using the first derivative of optical density of the thin films [50].

Figure 4.7 shows the absorption coefficient as a function of the photon energies. The sharp rise followed by 'hump' were observed. A sharp rise is observed in the absorption coefficient in the energy region from 1.35 eV o 1.65 eV. The 'hump' becomes significant as the crystallize size becomes smaller, exhibiting effective excitonic effects, as shown in figure 4.8. Moreover, a blue shift is clearly seen in the absorption edge. This behavior is explained in terms of quantum confinement effect in

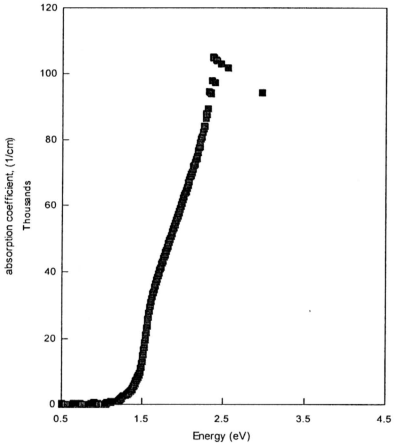

Figure 4.7 : Absorption spectrum of e-beam evaporated CdTe thin film

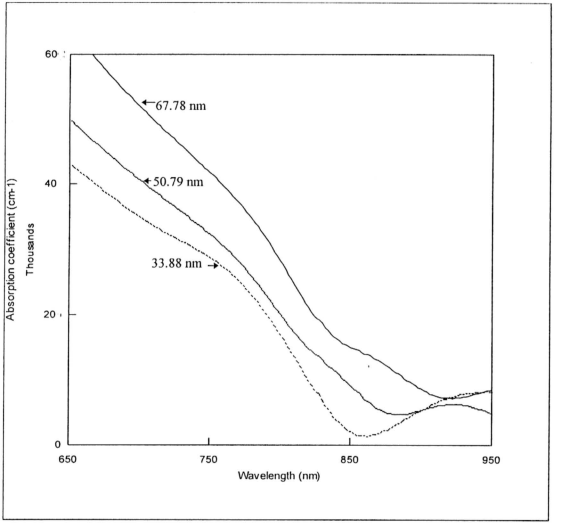

Figure 4.8 : Absorption spectra of CdTe

(A blue shift in the absorption edge is observed when the crystallite size decreases. The excitonic excitation levels becomes significant as the crystallite size reduces, which represented as 'hump' in the spectrum above)

the nanocrytallites, especially when their size is smaller than 4 times the Bohr radius [45] . Energy dependence of α near the band edge for band-to-band transitions (neglecting exciton effects) are given by [47]

$$\alpha(E) = A(E - E_g)^m \qquad \text{..... (4.24)}$$

where m = 0.5, 1.5 and 2 represent allowed direct, forbidden direct and indirect transitions respectively and A is linearity constant. Here we examined the relationship between the $(\alpha E)^2$ vs. E, $(\alpha E)^{1/2}$ vs. E and $(\alpha E)^{3/2}$ vs. E, where E is the energy in electron-volt and the respective diagrams are shown in figures 4. 9 (a), (b) and (c).
It is observed that only $(\alpha E)^2$ vs. E showed a linear dependence near the band edge. This indicates that the high absorption range takes place through direct interband transitions [111]. By extrapolating the linear region near the band edge, the band gap of the thin film can be estimated from the intercept on the energy axis. It was found that the films deposited have a band gap around 1.5 eV as reported by several researches [6,52,111]. In many films, the $(\alpha E)^2$ vs. E behaves parabolically that the determination of linear region to estimate band gap become more tedious and prone to errors. As an alternative, the first derivative of optical density was used to estimate the band gap. The transition was assumed to be direct allowed as found in this research and also as reported by other researches[6,111].

The optical density of thin film was used in the determination of the band gap . Optical density is taken to be [112]

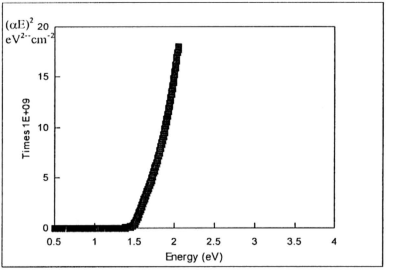

Figure 4.9 (a) : $(\alpha E)^2$ vs. E
(theoretical fitting for direct allowed band gap)

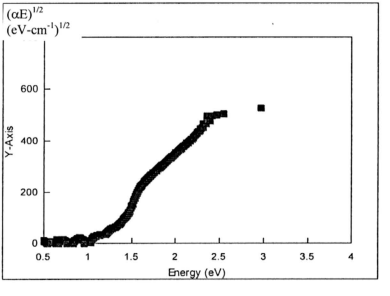

Figure 4.9 (b) : $(\alpha E)^{\frac{1}{2}}$ vs. E
(theoretical fitting for indirect band gap)

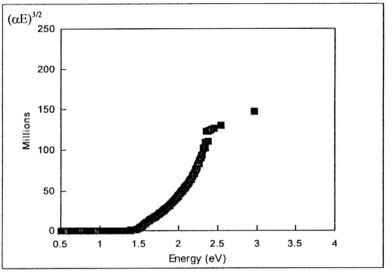

Figure 4.9 (c) : $(\alpha E)^{3/2}$ vs. E
(theoretical fitting for forbidden direct band gap)

$$Optical Density, O.D = \ln\left[\frac{(1-R)^2}{T}\right] \qquad \text{..... (4.25)}$$

where T is the transmittance and reflectivity, R is given as $(n-1)^2 / (n+1)^2$. The energy corresponding to a certain transition from the valence to conduction band which is

related the joint density of states critical point is observed to correspond to the low energy inflection point of the absorption onset [50].

By assuming the optical density as a function of photon energy, E, where

$$O.D = C_0 + C_1E + C_2E^2 + C_3E^3 + C_4E^4 + ... \qquad \text{..... (4.26)}$$

with C_0, C_1, C_2, C_3 and C_4 as constants. The constants were determined by regression analysis.

Figure 4.10 and 4.11 show the measured optical density and the fitted curve to determine C_0, C_1, C_2, C_3 and C_4.

The first derivative of the function is

$$\frac{d}{dE}(O.D) = C_1 + 2C_2E + 3C_3E^3 + 4C_4E^3 + ...$$

from which the transition energies corresponding to maxima in the spectrum are obtained. A typical spectrum is shown in figure 4.12. The peak of the first derivative of optical density correspond to the critical point in the joint density of electronic states $\nabla_k(E\text{-}E_0) = 0$ [112].

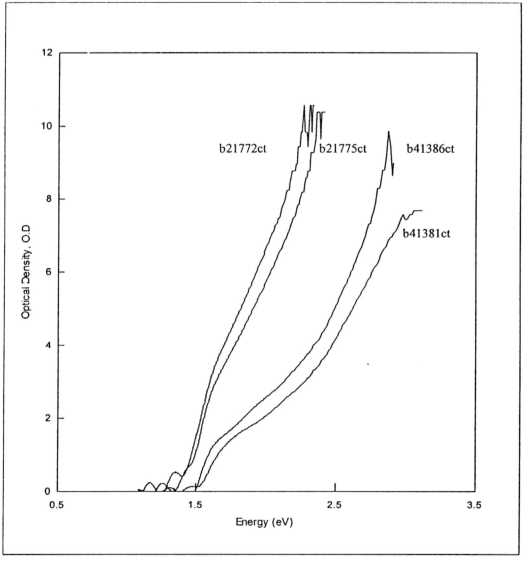

Figure 4.10 : Optical density of CdTe thin films.

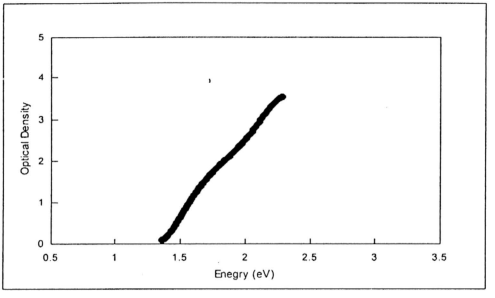

Figure 4.11 : Fitted optical density curve

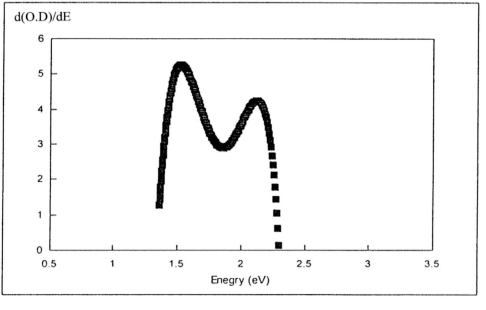

Figure 4.12 : First derivative of the fitted optical density curve

(the first peak corresponds to the direct allowed band gap of CdTe)

The peak observed at approximately 1.5 eV, correspond to the band gap, E_g, of the thin film. The values obtained via this method compare very well with the fitting of the α of the theoretical model of direct dipolar transitions between parabolic bands. The values are presented in table 4.5.

The calculated Eg was plotted against thickness as shown in figure 4.13. It is observed E_g increases with thickness. As for that the behavior was tried to link to the crystallite size, D_x, as D_x increases with thickness. But the attempt showed a random distribution of E_g suggesting that the shift is not entirely due to the crystallite size.

As mentioned above a deviation is seen in the band gap value of CdTe thin film from the single crystal CdTe value (1.499 eV) [4]. The deviation in the E_g can be attributed to the presence of stress in the material and the size effect of quantum origin produced by the microcrystalline nature of samples grown at low temperature [41].

CdTe thin films prepared are of microcrystalline nature with preferential growth of columnar type along the cubic [111] direction. Since the interplanar spacing along this direction was found to be smaller in 72 % of the samples than that of CdTe single crystal, it was interpreted as being the results of stress acting upon the CdTe lattice as highlighted in chapter 3. The estimated stress can be employed to calculate its contribution to the shift of Eg by using a theoretical approach that considers uniaxial stress along the direction [111] in semiconductor with zinc blende-type structures [113]. The existence of strain effect had been observed to cause the deviation in Eg in sputtered metallic films [114].

Table 4.5 : Estimated band gap values of CdTe thin films and the shift from single crystal band gap value.

sample	Band gap,E_g (eV)	Band gap shift, ΔE_g (eV)
b21771ct	1.532	0.033
b21772ct	1.526	0.027
b21773ct	1.527	0.028
b21774ct	1.531	0.032
b21775ct	1.541	0.042
b21777ct	1.53	0.031
b21778ct	1.539	0.040
b3861ct	1.547	0.048
b3862ct	1.553	0.054
b3863ct	1.576	0.077
b3864ct	1.552	0.053
b3865ct	1.568	0.069
b3686ct	1.591	0.092
b3687ct	1.562	0.063
b3688ct	1.563	0.064
b41381ct	1.567	0.068
b41382ct	1.595	0.096
b41383ct	1.596	0.097
b41384ct	1.568	0.069
b41385ct	1.581	0.082
b41386ct	1.600	0.105
b41387ct	1.601	0.106
b41388ct	1.571	0.072
b62591ct	1.574	0.075
b62592ct	1.541	0.042
b62593ct	1.542	0.043
b62594ct	1.591	0.092
b62595ct	1.592	0.093
b62596ct	1.495	0.000
b62597ct	1.548	0.049
b62598ct	1.528	0.029

[single crystal band gap value = 1.499 eV]

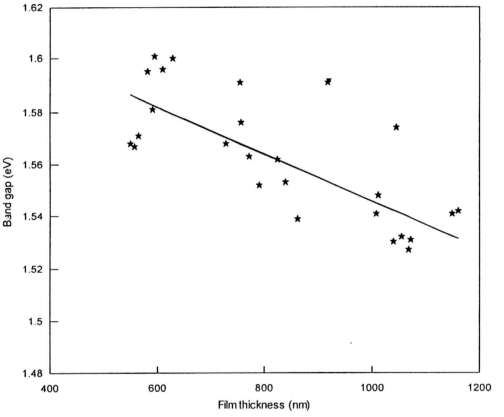

Figure 4.13 : Variation of band gap of CdTe with film thickness

(Band gap decreases with increasing film thickness ; fitted curve is shown as full line while the experimental points are represented by the stars.)

The value of E_g as a function of uniaxial strain parallel to the [111] direction in zinc blende-type semiconductor is, to first order in stress [113], given by

$$E^{[111]} = E_0 + \delta E_H - \frac{1}{2}\delta E_{[111]} \qquad \text{..... (4.27)}$$

where $\delta E_H = a(S_{11} + 2S_{12})S$; $\delta E_{[111]} = \frac{d}{3^{1/2}} S_{44} S$ and the shift in band gap due to stress,

$$\Delta E^{[111]} = \delta E_H - \frac{1}{2}\delta E_{[111]} \qquad \text{..... (4.28)}$$

In the expressions a and d are the deformation potentials. By substituting the deformation potential and elastic constants of CdTe as given in reference 66 and 115 respectively, the shift in band gap of a CdTe sample under uniaxial stress, S, were determined using the calculated stress values shown in table 3.3.

As indicated previously, quantum size effects may also have an important effect on the value of the energy gap of a microcrystallite semiconductor. It has been suggested that electron confinement may occur in films with small grain size, where grain boundaries play the role of potential barriers for electrons. This produces quantized levels in the conduction and valence bands resulting in a larger value for the fundamental transition [33,38,116-118]. Quantum size effects have also been observed in thin films of other materials such as CdSe [119-123], CdS [54] and more recently CdTe glass composite films [119].

The band shift caused by quantum size effects can be estimated using the effective mass model proposed by Brus [38]. Under the conditions the optical

transitions of an exciton are quantized and the energy shift of the first optical transition assuming parabolic energy band is given by

$$\Delta E_{shift} = \frac{h^2 \pi^2}{2R^2}\left[\frac{1}{m_e} + \frac{1}{m_h}\right] - \frac{1.786 e^2}{\epsilon R} - 0.24 E_{RY} \quad \text{..... (4.29)}$$

The first term in the above equation which is the quantum energy of localization of the charge carriers has a $1/R^2$ dependence where R is the radius of the crystallite. The second term which has 1/R is due to Coulomb interaction between the charge carriers while the last term represents spatial correlation effect where E_{RY} is the effective Rydberg energy, $\frac{e^4}{(2\epsilon h^2[m_e^{-1} + m_h^{-1}])}$

By assuming that the static dielectric constant and effective masses of electron and hole are respectively $0.2m_0$ [9], $0.11m_0$ and $0.3m_0$ [124], along the calculated crystallite size from XRD, the band shift was estimated. The variation of shift in band gap due to crystallite effect, ΔE_{crys}, is shown in figure 4.14.

The band gap shift obtained due to strain effect in the films, $\Delta E^{[111]}$ and due to quantum effects, ΔE_{crys}, were added to the single crystal CdTe band gap value and compared with the experimental value of E_g obtained via the method explained earlier.

According to this calculation, quantum size effects contribute noticeably to the increment of the band gap for crystallize sizes up to ~ 50 nm. However, majority of the samples prepared show the contribution in the shift due to quantum size-effect and strain effect is still below the band gap shift obtained experimentally (figure 4.15). This shows that there could be other mechanisms involved in the blue shift of the band edge. Researches have highlighted that the presence of different phases [41] could

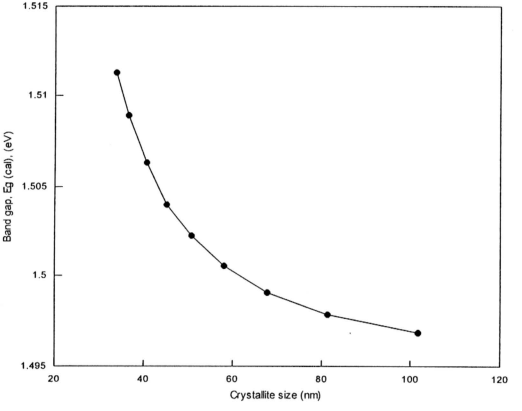

Figure 4.14 : Variation of bandgap with crystallite size
(The band gap was calculated using Brus model [50] using the crystallite radius obtained from the XRD data)

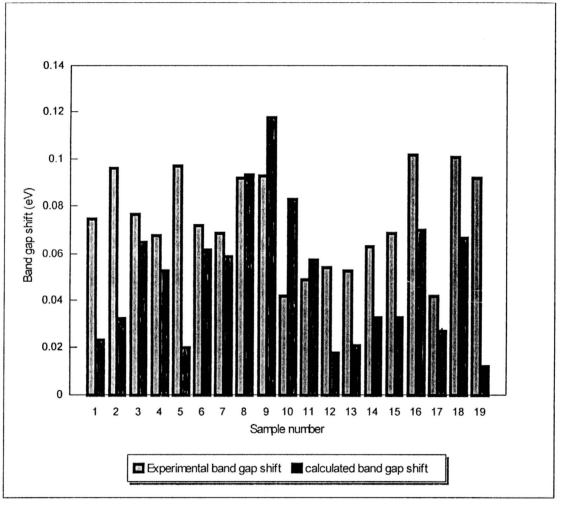

Figure 4.15 : Histogram showing the comparison between the calculated band gap shift and the experimental band gap shift.

(The calculated band gap shift could account for only up to ~ 60 % of the experimental band gap shift)

contribute to the shift. As no other phase than cubic was observed in this study, we propose that the presence of amorphous state CdTe as the background of the thin films prepared, may contribute to the shift. It has been reported [111] that amorphous CdTe has a larger band gap compared to single crystal. The films also rich in tellurium and it is suspected that the free tellurium in the material is the one forming the grain boundaries thus limit the potential well for the conducting electrons.

4.7 D.C. conductivity measurement

4.7.1. I-V measurement

Dark d.c. conductivity measurement at room temperature was carried out using 237 Keithley high voltage source measure unit up to 50 volts in both forward and reverse bias mode on Al/CdTe junctions. Figure 4.16 represents the I-V measurement carried out on five samples with varying thickness.

Only one distinct linear region was obtained throughout the measuring region as shown in the figure 4.16. The linear region was used to calculate the d.c.resistance of the e-beam evaporated CdTe thin films. Subsequently, the resistivity of these films were calculated from

$$\rho = \frac{RA}{l} \qquad \text{..... (4.28)}$$

where A is the area of conduction, which is given by the multiplication of film thickness and electrode width (= 4 mm) while l represents the distance between the two Aluminium planar electrodes. The values are presented in table 4.6.

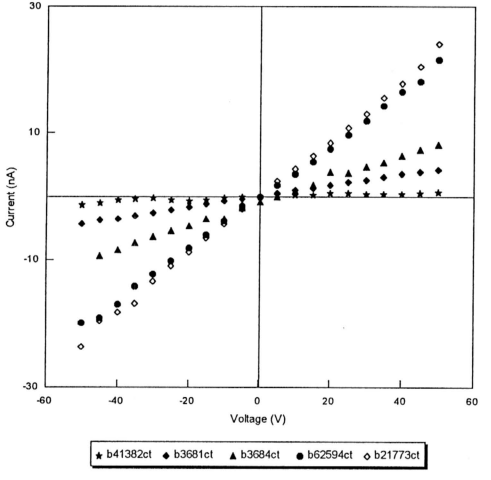

Figure 4.16 : I-V profile of e-beam evapotated CdTe thin films

Table 4.6 : Dark resistivity of e-beam evaporated CdTe thin film

sample	thickness, t (nm)	Resistance ($x10^{10}$ ohm)	Dark Resistivity, ρ ($x\ 10^6$ ohm-cm)
b41382ct	581	3.20	43.00
b3681ct	648.5	1.60	22.00
b3684ct	790	60.01	8.00
b62594ct	917.9	42.60	5.76
b21773ct	1069	42.70	5.70

The resistivity found ($\sim10^6$ - 10^7 ohm-cm) is large for semiconducting materials. It shows that the prepared CdTe thin films behave like semiconducting-semi insulating materials. High resistivity CdTe thin films was also obtained by other researches [60,125]. All their films were reported to contain excess Te for deposition below 473 K. As for that, the results obtained for the present study is not suprising as these films also have excess Te as had discussed before.

4.7.2. Effect of thickness on dark resistivity

Figure 4.17 represents the dependence of resistivity on film thickness. The distribution shows that the thin films have a varying resistivity with thickness unlike thickness-independent resisitivity in bulk materials of the same sample.

The profile obtained in the figure 4.17 shows clearly that the resistivity decrease rapidly with increasing thickness up to ~800 nm and then undergoes a gradual decrease. Similar observations have been reported for CdTe [8,60] and CdSe [73]. The variation of the resistivity can be correlated to the structural properties of the prepared films.

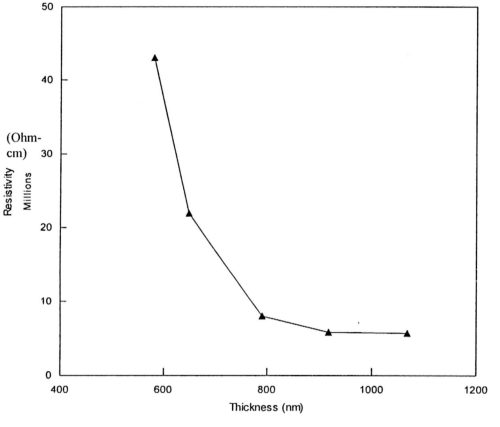

Figure 4.17 : Variation of resistivity with thickness

(A sharp decrease in the resistivity up to ~ 800nm followed up by a gradual decrease is observed)

The rapid decrease in resistivity up to ~ 800 nm probably due to the increase in the degree of preferred orientation [111] and the crystallite effect. The contribution of the crystallite size to the resistivity is negligible in this region of thickness as it is expected at small value of thickness, the fractional change of the size is very small. So, the predominant factor contributing to resistivity in small range is preferred orientation.

An abrupt increase in the fractional change of the size of crystallites in the range of large thickness, could account for the gradual decrease in film resistivity, apart from the degree of preferred orientation. The stoichiometry of the thin film has no or negligible effect on film resistivity as it was found that the stoichiometry was invaried with film thickness. Therefore the predominant factor in large range of thickness is crystallite size.

The behavior exhibited in the figure 4.17, for e-beam evaporated CdTe thin film is also attributed to the variation in the mobility which increases as the crystallite becomes larger in the thicker films [8,73].

The thickness dependence of resistivity is usually compared to Fuchs-Sondheimer (F-S) theory [126]. The theory predicts that

$$\rho_f = \rho_o\left[1+\frac{3l(1-p)}{8t}\right] \qquad \text{..... (4.31)}$$

where ρ_f and ρ_o are the resistivities of the film and the bulk material, l is the bulk mean free path and p is called the specularity parameter and characterizes the fraction of carriers that are secularly scattered at the surface. The F-S theory is applied on metals and based on free electron model. However the application on the investigated semiconducting films, showed there is no agreement with F-S theory as the plot ρt vs, t

did not yield a straight line as supported by other researches [127]. This contradicts the results reported by Ashour et.al. [60]. However, it seems that the agreement obtained in [60] is just a mathematical fit for the data obtained and it cannot give any physical meaning.